Opt Quant Electron (2007) 39:1009–1019
DOI 10.1007/s11082-007-9139-8

Integrating liquid crystal based optical devices in photonic crystal fibers

Thomas Tanggaard Alkeskjold · Lara Scolari · Danny Noordegraaf · Jesper Lægsgaard · Johannes Weirich · Lei Wei · Giovanni Tartarini · Paolo Bassi · Sebastian Gauza · Shin-Tson Wu · Anders Bjarklev

Received: 15 September 2007 / Accepted: 6 November 2007 / Published online: 24 November 2007

Abstract Liquid crystal photonic bandgap fibers form a versatile and robust platform for designing optical fiber devices, which are highly tunable and exhibit novel optical properties for manipulation of guided light. We present fiber devices for spectral filtering and polarization control/analysis.

Keywords Photonic crystal fibers · Fiber devices · Liquid crystals devices

1 Introduction

Photonic Crystal Fibres (PCFs) (Russell 2003), also known as microstructured optical fibers or holey fibers, have attracted worldwide interest within the last decade due to their unique optical properties and because they exhibit a much higher degree of design freedom compared to conventional optical fibers. These new and fascinating properties has fuelled the desire to make more efficient fiber lasers, light sources, dispersion compensating modules, optical sensors as well as new fiber devices using PCF technology (Eggleton et al. 2001; Kerbage et al. 2002; Knight et al. 1998; Bise et al. 2002; Larsen et al. 2003; Du et al. 2004). PCFs are characterized by an arrangement of micron-sized air holes running down the length of the fiber. The microstructure allows realization of the so-called index-guiding PCFs, which guide light in a high-index core using a principle similar to total internal reflection, and the Photonic BandGap (PBG) guiding PCFs (Knight et al. 1998), which can guide light in a low-index core. The unique properties of bandgap-guiding PCFs has opened the possibility

T. T. Alkeskjold (✉) · L. Scolari · D. Noordegraaf · J. Lægsgaard · J. Weirich · L. Wei · A. Bjarklev
COM•DTU, Department of Communications, Optics and Materials, Technical University of Denmark, Building 345v, Lyngby 2800, Denmark
e-mail: thomas@alkeskjold.dk

G. Tartarini · P. Bassi
DEIS, University of Bologna, Viale Risorgimento, 2, 40136 Bologna, Italy

S. Gauza · S. -T. Wu
College of Optics and Photonics, University of Central Florida, Orlando, FL 32816, USA

of combining the classical fiber material, silica, with new materials having higher refractive index than that of silica, and create guided wave structures for confinement of light in silica. This can be achieved by infiltrating the air holes of PCFs with liquid materials (Bise et al. 2002; Larsen et al. 2003; Alkeskjold et al. 2004; Zografopoulos et al. 2006; Lesiak et al. 2007; Haakestad et al. 2005; Scolari et al. 2005; Lægsgaard and Alkeskjold 2006; Alkeskjold et al. 2006; Steinvurzel et al. 2006; Yeom et al. 2007; Fuerbach et al. 2005; Noordegraaf et al. 2007; Alkeskjold and Bjarklev et al. 2007) in this way exploiting the tunability of liquids, while maintaining the compatibility and reliability of silica based optical fibers. A very interesting class of (liquid) materials for this purpose is the use of Liquid Crystals (LCs) as a mean of introducing enhanced tunability and controllability.

This paper gives an overview of the recent progress in Liquid Crystal Photonic BandGap (LCPBG) devices, which allow for thermally, electrically, and all-optically tuning of a range of in-fiber components such as spectral filters, polarizers and polarization controllers.

2 Liquid crystal photonic bandgap devices

Liquid crystals are organic molecules, which can exhibit very high electro-optic and thermo-optic effects due to a high birefringence (up to 0.5) and high dielectric anisotropy (up to $50\varepsilon_0$) as well as the presence of phase transitions—giving a dn/dt of up to 10^{-2} (Li et al. 2004). If infiltrated and aligned correctly in a solid-core PCF, having a periodic arrangement of air holes in the cladding as shown on Fig. 1, the fiber will switch from being an index-guiding type to a bandgap guiding type, where light is guided by anti-resonant reflections from the cladding structure (Litchinitser et al. 2004; Lægsgaard 2004). Light within certain wavelength bands will be confined to the core of the fiber—observed as pass bands in the transmission spectrum. This is illustrated on Fig. 2, which shows the effective mode indices of the upper three bands of supermodes in a triangular structured PCF with a hole diameter of $3\,\mu$m, an inter hole distance of $7\,\mu$m (see Fig. 1) and air holes infiltrated with a high-index isotropic liquid ($n = 1.5025$). The first three bands consist of coupled LP_{01}, LP_{11} and LP_{21}-like modes that are confined to the high-index rods (the capillary holes filled with liquid). These modes form narrow bands of modes separated by a small gap in effective index (the band gap). The core acts as a defect and supports a guided mode with an effective index less than that of the background material (silica $n = 1.445$). The mode is in this case guided within the bandgap from approximately 1.07 to $1.6\,\mu$m wavelength. Within the bandgap, the mode is guided by reflections from the periodically spaced high index rods surrounding the core, and cannot couple to the cladding modes because of a high index difference between the guided mode and the cladding supermodes. At wavelengths where the effective index of the supermodes is equal to the background index, the core mode will no longer be guided and stop bands occur in the transmission spectrum. These stop bands corresponds to the cut-off wavelength of the modes present in an isolated high-index rod and can be approximated as (Litchinitser et al. 2004):

$$\lambda_m = \frac{2d\sqrt{n_1^2 - n_2^2}}{m + \frac{1}{2}} \tag{1}$$

where d is the hole diameter, n_1 and n_2 are the refractive indices of the filling and background material, respectively, and m is an integer referring to the m^{th} cut-off wavelength.

Depending on the alignment of the LC in the capillaries, the anisotropy of the LC will have a more or less significant influence on the bandgaps and even causes new bandgaps

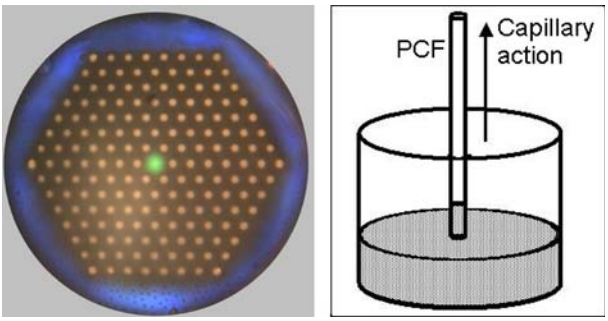

Fig. 1 Micrograph of the end facet of a liquid crystal infiltrated PCF guiding green light due to the PBG effect (left), the PCF is filled using capillary action (right)

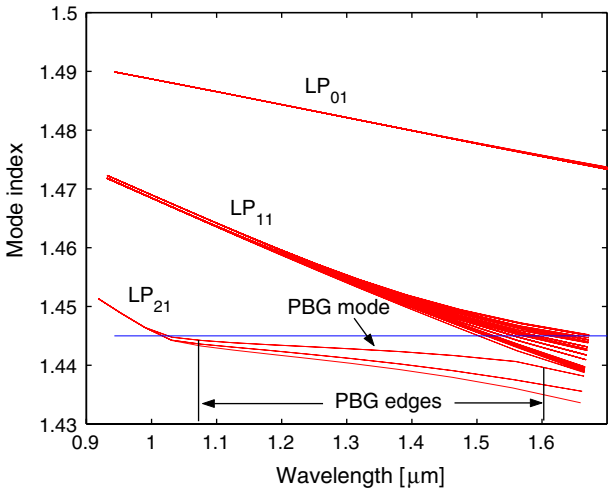

Fig. 2 Simulated effective mode indices of the modes in a triangular structured PCF with n=1.5025 isotropic high index filled cladding holes

to appear simply due to the high optical anisotropy. Figure 3 shows the same simulation as shown on Fig. 2 but with an anisotropic tensor profile with $n_x = n_y = 1.5025$ and $n_z = 1.67$, which corresponds to a planar aligned nematic LC such as E7 from Merck. Due to the anisotropy, the effective mode index of the LP_{21} manifold increases slightly causing a 100 nm red shift of the short wavelength PBG edge—effectively narrowing the width of the bandgap by 100 nm. Furthermore, the LP_{11} manifold (TE_{01}, TM_{01} and HE_{21}) splits up and a small gap between them is formed. In some cases, this gap can support guided modes simply by the anisotropic splitting of isotropic degenerate modes (Alkeskjold et al. 2006). This splitting occurs because the TE_{01}, TM_{01} and HE_{21} modes have different distribution of their electric field, which is therefore affected differently by the anisotropy. Figure 4 shows an experimental observed transmission spectrum from a PCF (LMA10, Crystal Fibre) infiltrated over a length of 10 mm with the nematic LC E7 from Merck. The LC is in this case planar aligned i.e., with the director along the fiber. The red vertical lines mark the calculated cut-off wavelengths of the modes in a single (anisotropic) cylindrical LC infiltrated waveguide, and predicts the stop bands of the fiber.

The narrow bandgap around 1100 nm appears due to the anisotropic splitting of the HE_{12} and EH_{11} mode, which are degenerate in the isotropic case. Also, the gap at 790 nm appears

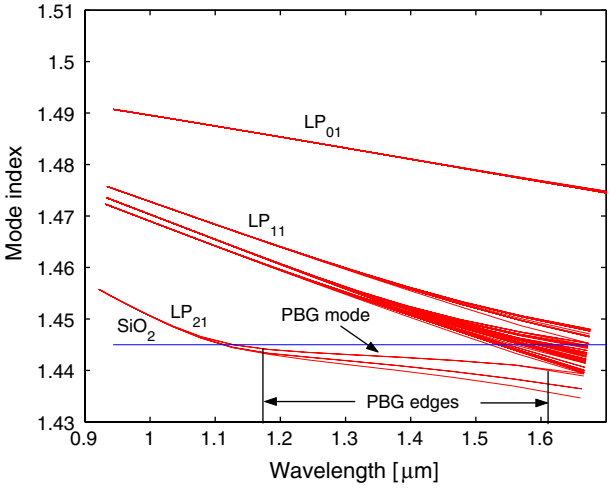

Fig. 3 Simulated effective mode indices of the modes in a triangular structured PCF with $n_x = n_y = 1.5025$ and $n_z = 1.67$ high index filled cladding holes

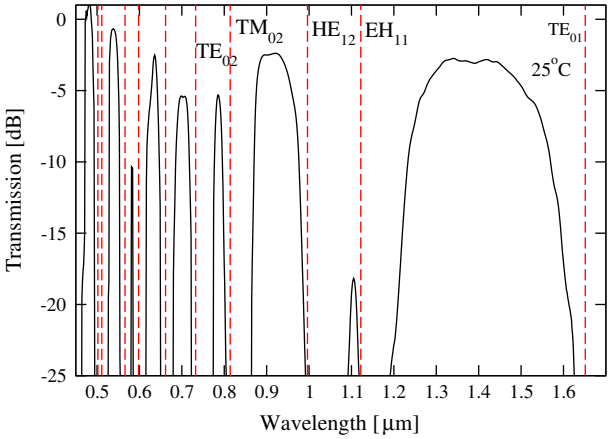

Fig. 4 Experimental observed transmission spectrum of a LMA10 PCF (Crystal Fibre) infiltrated with E7 (Merck). The spectrum is measured at 25°C and normalized to the spectrum of an unfilled PCF. Vertical dashed lines indicate the modal cut-offs of a single LC rod and predicts the stop bands of the fiber

due to anisotropic splitting of the TE_{02} and TM_{02} mode. The splitting occurs because the electric field of the TE_{02} mode is in the transversal direction, while part of the electric field of the TM_{02} is also in the longitudinal direction, i.e., along the extra-ordinary index of the LC.

The spectral position of the bandgaps is very sensitive to the optical properties of the LC i.e., refractive indices and orientation/alignment. The bandgaps are therefore easily tuned by manipulating the LC using external electric fields (Haakestad et al. 2005; Scolari et al. 2005; Noordegraaf et al. 2007; Alkeskjold and Bjarklev et al. 2007), varying the temperature (Larsen et al. 2003; Lesiak et al. 2007; Lægsgaard and Alkeskjold 2006; Alkeskjold et al. 2006) or utilizing the absorption of a guided pump beam in a dye doped LC (Alkeskjold et al. 2004).

3 Tunable birefringence

Having electrical control of the orientation of the LC molecules in LCPBG devices is in many applications very useful, because the refractive index can be adjusted in a much wider range than by using thermal or optical means of tuning. Also, applying an external electric field breaks the six-fold symmetry of the fiber and induces a polarization dependence of the transmission, which is not present when using thermal and optical methods, unless the symmetry is broken by structural variation such as elliptical holes (Tartarini et al. 2007). This can be very useful in devices for filtering or manipulating the polarization of the transmitted light.

The characteristics of devices having planar aligned LCs, are the presence of an electric field threshold called the Fredericks transition threshold. Below the threshold the dielectric torque, induced by the field acting on the LC molecules, is lower than the elastic torque keeping the molecules planar aligned and the LC will stay planar aligned. However, when the dielectric torque is higher than the elastic torque, the LC molecules will start to reorient towards being parallel or perpendicular to the field, depending on the sign of the dielectric anisotropy. Furthermore, when the LC molecules start reorienting, domains with reverse tilt start to appear and these create polarization dependent scattering (Haakestad et al. 2005). Figure 5 shows the formation of reverse tilt domain defects.

A very common technique for reducing the threshold effect and the associated reverse tilt domains is to provide a small (a few degrees) pretilt to the mesogens at the surface, using a surface coating and a rubbing technique. This way, a preferred direction of reorientation is defined. This method is very impractical in capillaries and fibers, but a pretilt of 45° can be obtained by using a so-called dual-frequency LC (MDA-00-3969 from Merck), which have the alignment shown on Fig. 6.

Furthermore, the dual frequency property of MDA-00-3969 means that the dielectric anisotropy is positive at low frequencies (1 kHz) but is negative at higher frequencies (50 kHz) with a cross-over frequency at approximately 15 kHz. This means that low-frequency fields

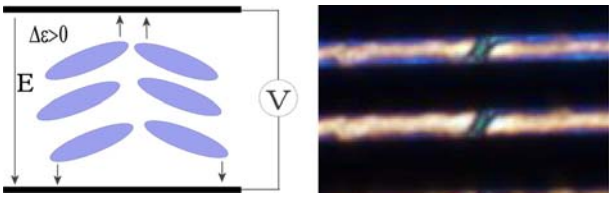

Fig. 5 Illustration of a reverse tilt domain defect, where the LC molecules reorient in opposite direction as a response to the field (left) and polarized micrograph of a reverse tilt domain defect in a LC filled capillary (right)

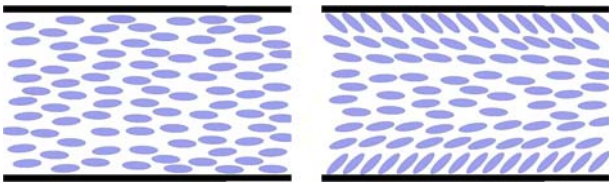

Fig. 6 Molecular orientation of a planar alignment (left) and a splayed alignment (right), where the molecules have an angle of 45° at the surface and bends towards the center, where it is parallel

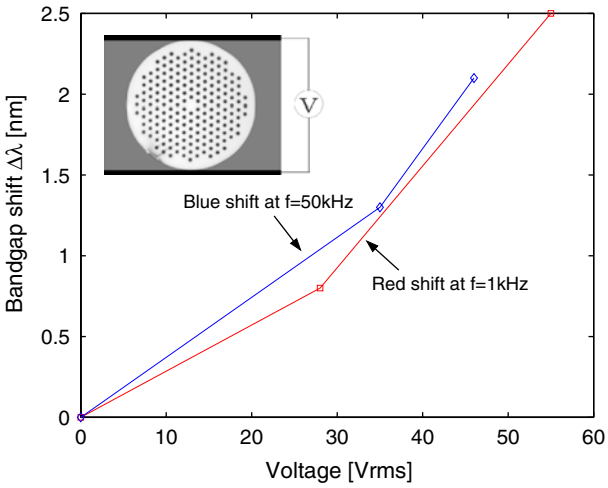

Fig. 7 Frequency controlled red and blue shift of the bandgap as a function of applied voltage. Inset shows the PCF sandwiched between the two electrodes used to drive the device

will induce a dielectric torque, which reorients the molecules toward being parallel to the electric field. For high-frequency fields the dielectric torque is perpendicular to the low-frequency torque and will orient the molecules toward being perpendicular to the electric field.

Using this principle, the bandgaps can be both red- and blue-shifted depending on which frequency is applied to the electrodes (Scolari et al. 2005). Figure 7 plots the red and blue shift of a short-wavelength bandgap edge around 1550 nm wavelength as a function of frequency and voltage. The shift of the bandgap edge is polarization sensitive because the symmetry of the fiber is reduced to two-fold when the field is applied. Then, the two guided modes lose their degeneracy and the fiber becomes birefringent. Figure 8 plots the measured birefringence induced by the field as function of applied voltage (Scolari et al. 2005). The inset shows the rotation of the state of polarization of 1600 nm light when 96 Vrms is applied to the fiber, demonstrating that the fiber acts as a tunable waveplate used in many modern polarization controllers for telecom applications. In this experiment, the fiber has a hole diameter of 5 μm, an inter hole distance of 10 μm and an outer diameter of 125 μm (LMA15, Crystal Fibre). Please see (Scolari et al. 2005) for further details.

4 Dynamic fiber grating devices

Modern fiber grating devices are widely deployed in areas such as add-drop filters in telecom systems, gain equalization of optical amplifiers, strain and stress sensors in buildings, and many more. Most gratings are static gratings, i.e., gratings with properties defined during the fabrication process of the grating. This causes some limitations in certain applications such a gain equalization of fiber amplifiers in dynamic networks. On the other hand, the properties of dynamic gratings can be altered and tuned continuously to the desired properties and, therefore, continuously adjusted to optimum performance in a dynamic environment. Therefore dynamic fiber gratings will be preferable in some applications.

Dynamic Long Period Gratings (LPGs) can easily be formed in LCPBG fibers simply by applying a periodic stress using a threaded rod or by applying a periodic electric field (Noordegraaf et al. 2007) using a comb electrode as shown in the inset on Fig. 9. The comb

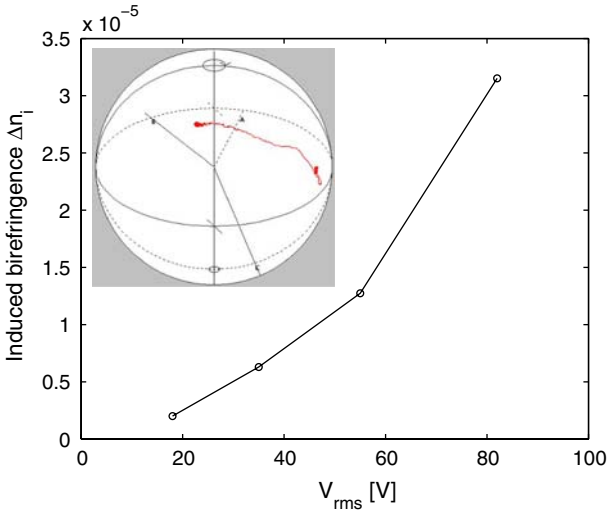

Fig. 8 Voltage controlled birefringence at 1 kHz field frequency. Inset shows the Poincaré sphere and the polarization rotation occurring when 96 Vrms voltage is applied

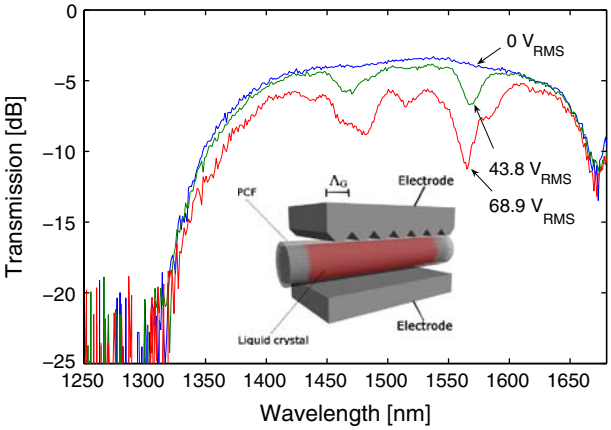

Fig. 9 Long period grating resonances induced in a LCPBG fiber using a comb electrode

electrode is preferable because it allows the grating to be electrically induced instead of being mechanically induced. The comb electrode causes the LC molecules to reorient periodically—effectively inducing a grating with a period corresponding to the period of the comb electrode. The grating acts as a notch-type filter, which can filter out a narrow wavelength band. At the notch wavelength, the core mode will couple to a lossy co-propagating cladding mode, which fulfills the phase matching condition:

$$\lambda_r = \Lambda(n_c - n_{cl}) \tag{2}$$

where λ_r is the resonance wavelength, n_c and n_{cl} are the effective indices of the core and cladding mode, respectively, and Λ is the period of the grating.

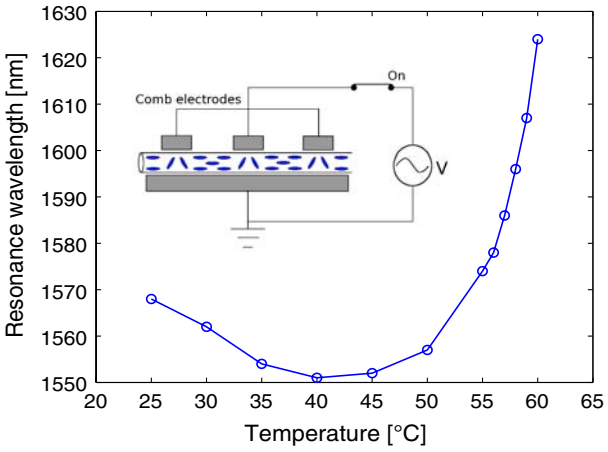

Fig. 10 Temperature tuning of the LPG resonance wavelength. Inset illustrates how the comb electrode reorients the LC molecules

Figure 9 plots the bandgap transmission spectrum of a LCPBG fiber (LMA10 with E7) placed between two electrodes, where the top electrode is periodically cut with an 800 μm groove period. The figure shows that several resonance notches appear in the transmission spectrum when a voltage is applied to the electrodes. The presence of multiple resonance wavelengths indicates that the core mode couples to several different closely spaced cladding modes and our simulation confirm this (Noordegraaf et al. 2007). The effective index of these cladding modes is highly sensitive to the refractive index of the LC, which can be tuned by increasing or decreasing the temperature of the device. By varying the index of the cladding mode, the phase matching condition changes and the resonance wavelength also varies. Figure 10 plots the temperature sensitivity of one of the resonance wavelengths and demonstrates that the resonance wavelength can be tuned from 1550 to 1620 nm over only 20°C. The inset illustrates how the LC molecules in the PCF are reoriented by the electric field between the comb electrode and the substrate electrode.

5 Switchable and rotatable polarizer

Since an external applied electrical field breaks the symmetry of the LCPBG fiber structure and thereby induces polarization dependence, it is desirable to control the electric field in a more flexible way in order to control the optical axis of the device. Figure 11 shows a recently demonstrated device structure (Alkeskjold and Bjarklev et al. 2007) where the LCPBG fiber is mounted in a double V-groove assembly fabricated in a silicon substrate. Gold electrodes are deposited on the side walls of the grooves, forming a set of electrodes, which fixes the fiber at four orthogonal corners relative to the core. The electrodes are electrically isolated from the silicon substrate by a thin layer of thermal oxide (SiO_2) and a thin layer of titanium is used as an adhesion layer between the gold and the oxide. The device is assembled by placing a 10 mm long solid-core PCF (LMA10, Crystal Fibre) infiltrated with LC E7 (Merck), containing, on the bottom V-groove section, one pair of electrodes, an integrated resistive heater, and an electrode for resistivity monitoring of the device temperature. The bottom section is 20 mm long and 5 mm wide. Two SMF28 fiber pigtails are fixed in the groove at each end of the LCPBG fiber for coupling in and out of the device. A top lid containing a V-groove with the second pair of electrodes is placed on top of the fibers and fixes the fibers in

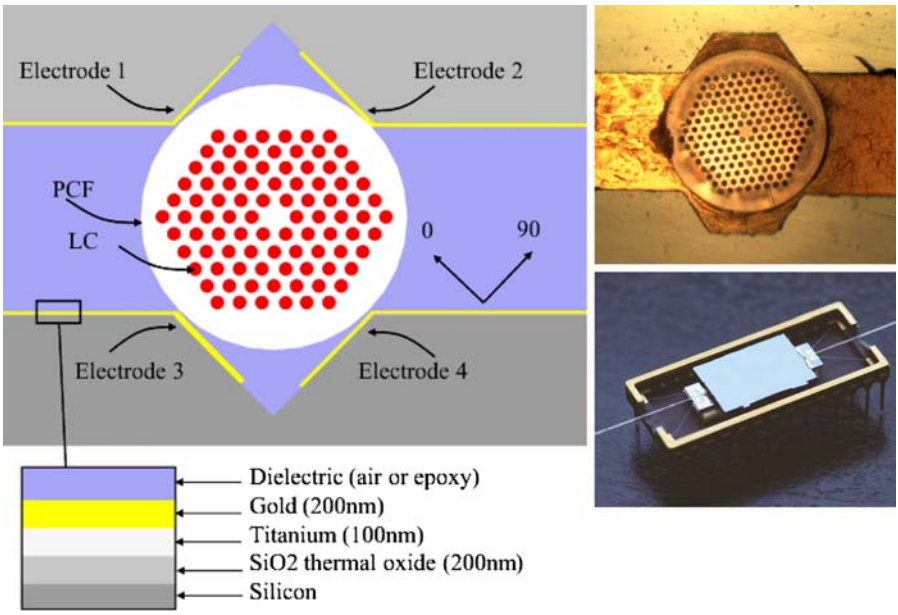

Fig. 11 Schematic view of the device (left) and micrograph of the fabricated device (top right). The device is pigtailed using two SMF28 fibers and mounted in a package and wire bonded for electrical access (bottom right)

the grooves. Finally, the assembly is sealed with epoxy. The device is annealed by elevating the temperature to 70°C and cooled down slowly to achieve a homogeneous planar alignment of the LC. Figure 11 (right, top) shows a micrograph of the fabricated device, where the PCF is mounted in the V-groove assembly and sealed with epoxy for polishing purposes. Figure 11 (right, bottom) shows the device mounted in a ceramic package with electrical connections.

Using the four electrodes it is possible to control the direction of the electric field in the transversal direction and thereby also the transversal orientation of the LC molecules, in this way obtaining one more degree of freedom in controlling the device. Figure 12 shows the transmission spectrum when no field is applied as well as the polarization dependent transmission spectrum when ± 39 Vrms is applied to electrode 2 and 3 of Fig. 11, respectively, and 0 V is applied to electrode 1 and 4 of Fig. 11. When the field is applied, the transmission becomes highly polarization sensitive–acting as a polarizer having a transmission axis orthogonal to the direction of the electric field. By controlling the electrodes independently, the direction of the electrical field can be rotated and effectively rotating the optical axis of the polarizer.

The increased loss of the optical mode polarized along the electrical field direction is caused by a combination of two effects: first, the effective mode index of the cladding states belonging to the short wavelength bandgap edge mode (the EH11 mode) is pushed up and into the bandgap, causing polarization-dependent coupling of the core mode to this cladding state. This is observed as a slight red shift of the bandgap shown on Fig. 12.

Second, the reorientation of the LC molecules along the field direction causes polarization-dependent scattering appearing from reverse tilt domain defects of the LC (Haakestad et al. 2005). These defects occur on an average longitudinal spacing of 100 μm in each of the capillaries nearest to the active electrodes, experiencing an electric field strength above the Fre-

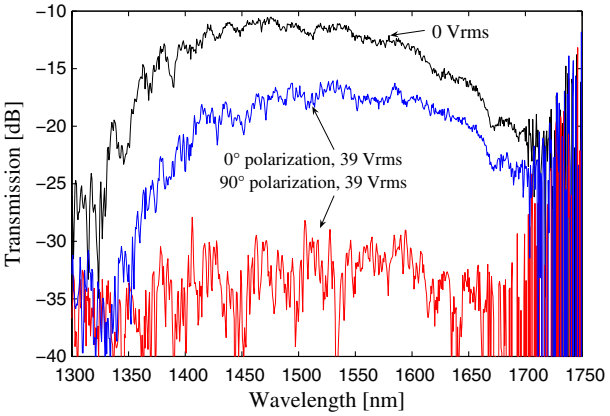

Fig. 12 The curves show the experimentally observed transmission spectrum when no field is applied as well as the polarization dependent transmission spectrum when ±39 Vrms is applied to electrode 2 and 3 of Fig. 11

Fig. 13 Polarization extinction ratio and activation loss as function of applied voltage

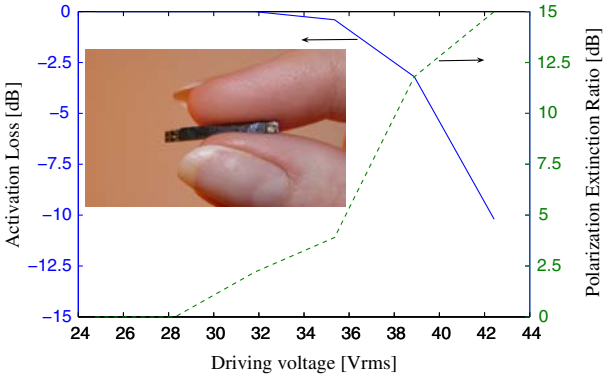

dericks transition of the LC. Figure 13 plots the activation loss and the polarization extinction ratio of the polarizer as a function of applied voltage. The polarization extinction ratio can be switched from 0 to 15 dB for a 10 mm long device. The inset shows a picture of the device and illustrates the physical size of the device.

6 Concluding remarks

Photonic crystal fibers is an interesting and promising host for infiltrating liquid crystals for creating tunable fiber devices operating by the photonic bandgap effect. These fibers have many new and interesting properties, which may be useful in applications requiring tunable properties such as tunable spectral filtering and/or polarization control and analysis. Many different devices have been demonstrated and proposed ranging from a highly birefringent fiber, a tunable waveplate, a switchable polarizer, light choppers, bragg switches, tunable grating filters, fibers with tunable polarization mode dispersion and several thermally tunable spectral filters for applications such as optical coherence tomography. Common for all these devices is that they are very compact, robust and can be integrated in a small size package

such as the double V-groove platform described in this paper—forming a low-cost component technology.

Acknowledgements Dr. T. T. Alkeskjold is supported by the Danish Research Council, Grant No. 274-06-0253

References

Alkeskjold, T.T., Bjarklev, A.: Electrically controlled liquid crystal photonic bandgap fiber polarimeter. Opt. Lett. **32**(12), 1707–1709 (2007)

Alkeskjold, T.T., Lægsgaard, J., Bjarklev, A., Hermann, D., Anawati, A., Broeng, J., Li, J., Wu, S.T.: All-optical modulation in dye-doped nematic liquid crystal photonic bandgap fibers. Opt. Express **12**, 5857–5871 (2004)

Alkeskjold, T.T., Lægsgaard, J., Hermann, D., Broeng, J., Li, J., Gauza, S., Wu, S.T., Bjarklev, A.: Highly tunable large-core liquid crystal photonic bandgap fiber. Appl. Opt. **45**, 2261–2264 (2006)

Bise, R.T., Windeler, R.S., Kranz, K.S., Kerbage, C., Eggleton, B.J., Trevor, D.J., et al.: Tunable photonic band gap fiber. Optical fiber communication conference technical digest, pp. 466–468 (2002)

Du, F., Lu, Y.Q., Wu, S.-T.: Electrically tunable liquid-crystal photonic crystal fiber. Appl. Phys. Lett. **85**, 2181–2183 (2004)

Eggleton, B.J., Kerbage, C., Westbrook, P.S., Windeler, R., Hale, A.: Microstructured optical fiber devices. Opt. Express **9**, 698–713 (2001)

Fuerbach, A., Steinvurzel, P., Bolger, J., Eggleton, B.J.: Nonlinear pulse propagation at zero dispersion wavelength in anti-resonant photonic crystal fibers. Opt. Express **13**, 2977–2987 (2005)

Haakestad, M.W., Alkeskjold, T.T., Nielsen, M.D., Scolari, L., Riishede, J., Engan, H.E., Bjarklev, A.: Electrically tunable photonic bandgap guidance in a liquid-crystal-filled photonic crystal fiber. IEEE Photon. Technol. Lett. **17**, 819–821 (2005)

Kerbage, C., Windeler, R.S., Eggleton, B.J., Mach, P., Dolinski, M., Rogers, J.A.: Tunable devices based on dynamic positioning of micro-fluids in micro-structured optical fiber. Opt. Commun. **204**, 179–184 (2002)

Knight, J.C., Broeng, J., Birks, T.A., Russell, P.St.J.: Photonic bandgap guidance in optical fibers. Science **283**, 1476–1478 (1998)

Lægsgaard, J.: Gap formation and guided modes in photonic bandgap fibres with high-index rods. J. Opt. A Pure Appl. Opt. **6**, 798–804 (2004)

Lægsgaard, J., Alkeskjold, T.T.: Designing a photonic bandgap fiber for thermo-optic switching. J. Opt. Soc. Am. B **23**, 951–957 (2006)

Larsen, T.T., Bjarklev, A., Hermann, D.S., Broeng, J.: Optical devices based on liquid crystal photonic bandgap fibres. Opt. Express **11**, 2589–2596 (2003)

Lesiak, P., Wolinski, T.R., Brzdakiewicz, K., Nowecka, K., Ertman, S., Karpierz, M., Domanski, A.W., Dabrowski, R.: Temperature tuning of polarization mode dispersion mode dispersion in single-core and two-core photonic liquid crystal fibers. Opto-Electron. Rev. **15**, 27–31 (2007)

Li, J., Gauza, S., Wu, S.-T.: High temperature-gradient refractive index liquid crystals. Opt. Express **12**, 2002–2010 (2004)

Litchinitser, N.M., Dunn, S.C., Steinvurzel, P.E., Eggleton, B.J., White, T.P., McPhedran, R.C., Sterke, C.M.de : Application of an ARROW model for designing tunable photonic devices. Opt. Express **12**, 1540–1550 (2004)

Noordegraaf, D., Scolari, L., Lægsgaard, J., Rindorf, L., Alkeskjold, T.T.: Electrically and mechanically induced long period gratings in liquid crystal photonic bandgap fibers. Opt. Express **15**, 7901–7912 (2007)

Russell, P.St.J.: Photonic crystal fibers. Science **299**, 358–362 (2003)

Scolari, L., Alkeskjold, T.T., Riishede, J., Bjarklev, A., Hermann, D., Anawati, A., Nielsen, M., Bassi, P.: Continuously tunable devices based on electrical control of dual-frequency liquid crystal filled photonic bandgap fibers. Opt. Express **13**, 7483–7496 (2005)

Steinvurzel, P., Moore, E.D., Mägi, E.C., Kuhlmey, B.T., Eggleton, B.J.: Long period grating resonances in photonic bandgap fiber. Opt. Express **14**, 3007–3014 (2006)

Tartarini, G., Pansera, M., Alkeskjold, T.T., Bjarklev, A., Bassi, P.: Polarization properties of elliptical hole liquid crystal photonic bandgap fibres. IEEE J. Lightw. Tech. **25**, 2522–2530 (2007)

Yeom, D.-I., Steinvurzel, P., Eggleton, B.J., Lim, S.D., Kim, B.Y.: Tunable acoustic gratings in solid-core photonic bandgap fiber. Opt. Express **15**, 3513–3518 (2007)

Zografopoulos, D.C., Kriezis, E.E., Tsiboukis, T.D.: Tunable highly birefringent bandgap-guiding liquid crystal microstructured fibers. J. Lightwave Tech. **24**, 3427–3432 (2006)